Supplementary Information

Effects of Humic and Fulvic Acids on Silver Nanoparticle Stability, Dissolution, and Toxicity

Ian L. Gunsolus, Maral P. S. Mousavi, Kadir Hussein, Philippe Bühlmann, and Christy L. Haynes**

Department of Chemistry, University of Minnesota, 207 Pleasant Street SE, Minneapolis, Minnesota 55455, United States

Fax: 612-626-7541, 612-626-7541 Tel: 612-626-1096, 612-624-1431

E-mail: chaynes@umn.edu, buhlmann@umn.edu

Contents

Characterization of AgNPs by TEM and Zeta-potential Measurements:

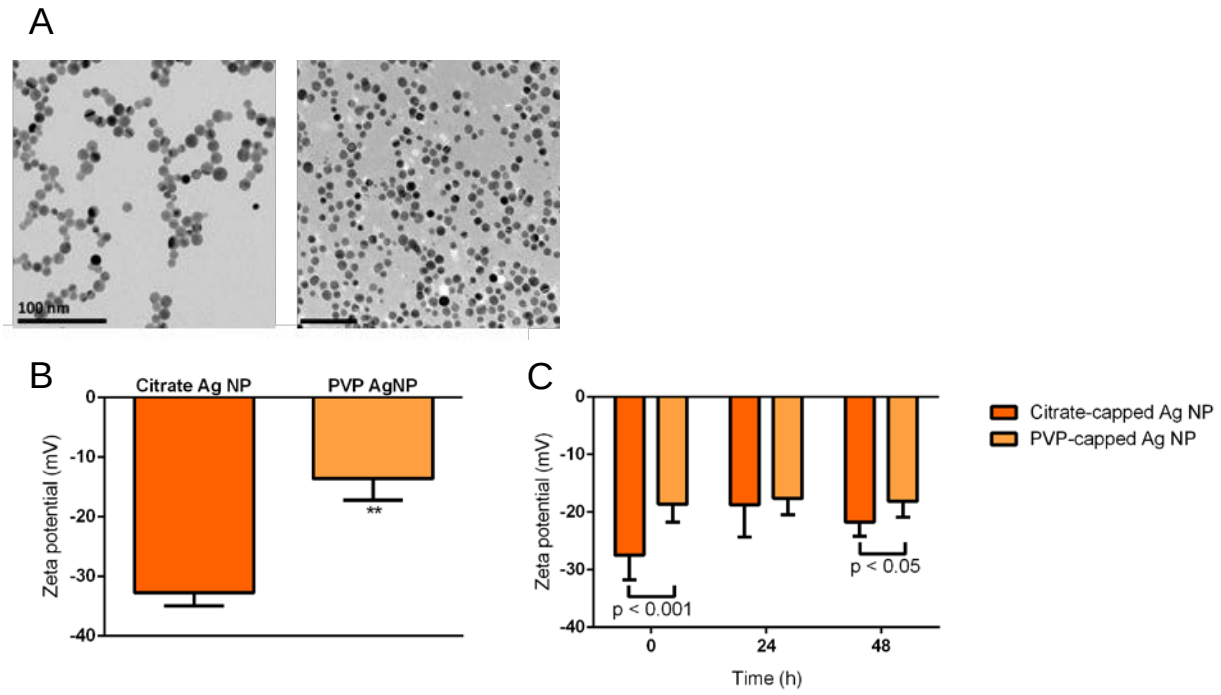

Figure S1. A: TEM micrographs of citrate-capped AgNPs (top left) and PVP-capped AgNPs (top right) reveal no change in nanoparticle size following exchange of the capping agent. B: Zeta potentials of freshly prepared AgNPs in deionized water (pH 6), where citrate- and PVP-capped AgNPs have average zeta potentials of -32.8 ± 2.2 mV and -13.6 ± 3.6 mV. Error bars represent the standard deviation of three independent replicates, each consisting of three zeta-potential measurements. Asterisks indicate $p < 0.01$ as calculated by the unpaired t-test. C: Stability of citrate- and PVP-capped AgNP zeta potentials over 48 h in deionized water (pH 6). P values shown were calculated by the unpaired t-test.

Aggregation of Citrate-capped AgNPs in a High Ionic Strength Buffer Containing 10 mg/L NOM Observed by UV-vis Extinction Spectroscopy:

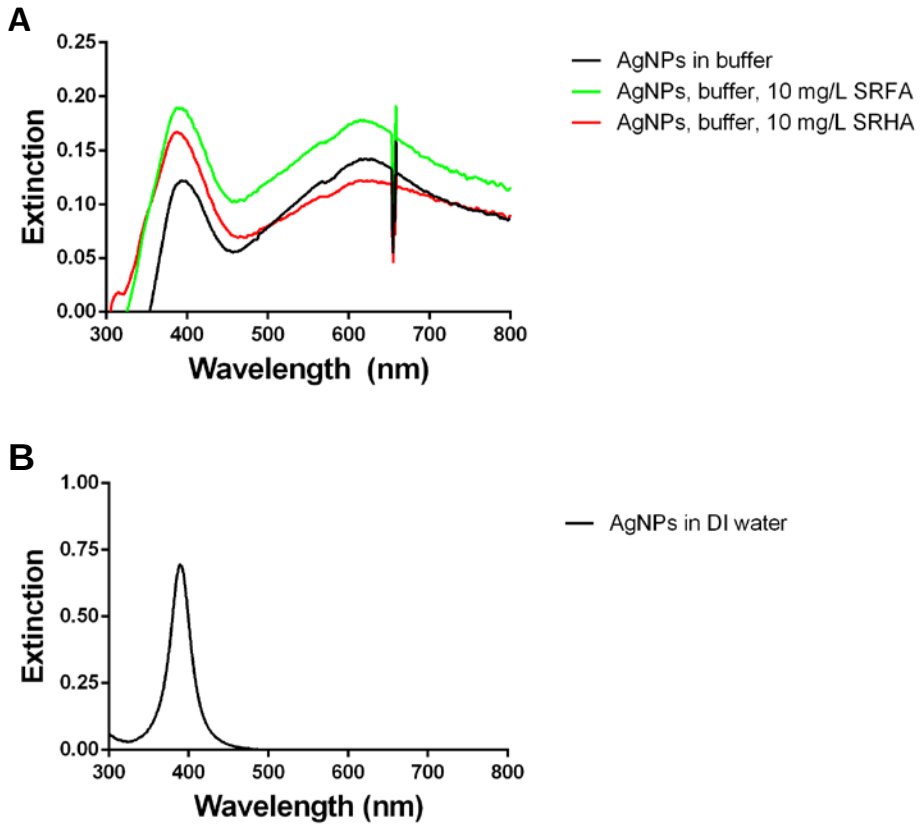

Figure S2. A: UV-vis extinction spectroscopy indicates that the addition of 10 mg/L NOM to a 0.1 M ionic strength phosphate buffer does not stabilize the AgNPs against homoaggregation, since the broad peak with maximum near 620 nm, attributable to variable-sized AgNP aggregates, is present in samples with and without NOM. Spectra of citrate-capped AgNPs exposed to no NOM, 10 mg/L Suwannee River Fulvic Acid (SRFA), or 10 mg/L Suwannee River Humic Acid (SRHA) in pH 7.5 phosphate buffer are shown. The feature observed near 670 nm is an instrumental artifact. B: Prior to AgNP introduction to the high ionic strength buffer with or without NOM, the extinction spectrum showed a single peak centered at 391 nm, indicative of a lack of aggregates and a relatively narrow particle size distribution. A representative spectrum is shown.

NOM Elemental Composition:

	C	H	O	N	S
Suwannee River Humic Acid Standard II	52.63	4.28	42.04	1.17	0.54
Suwannee River Fulvic Acid Standard II	52.34	4.36	42.98	0.67	0.46
Pony Lake Fulvic Acid Reference	52.47	5.39	31.38	6.51	3.03

Table S1. Elemental compositions of the three NOM models used in this study. Values shown are the percent (w/w) content of a dry, ash-free NOM sample.[2]

Dark-field Microscopy and Hyperspectral Imaging Characterization of Citrate-capped AgNPs Exposed to NOM:

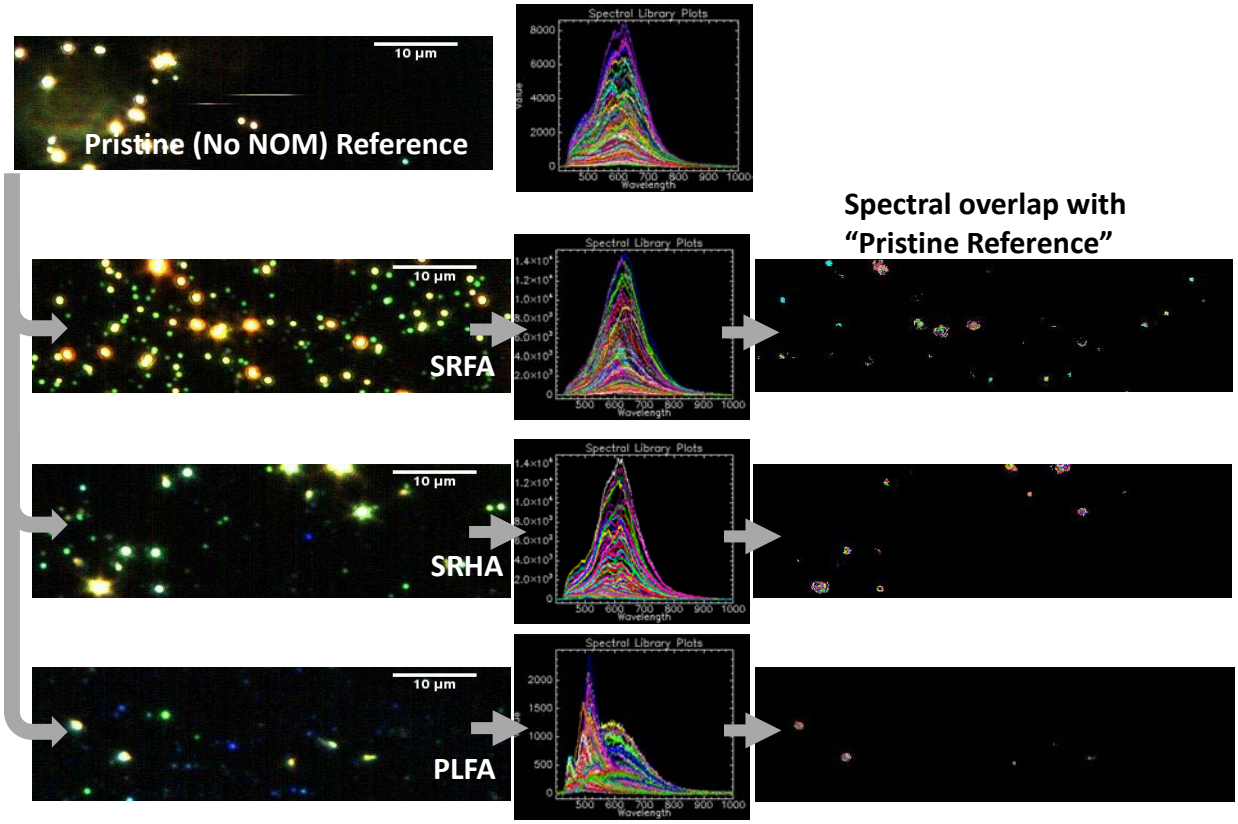

Figure S3. NOM-stabilized AgNPs are shown in order of increasing similarity (bottom to top on the right) to AgNPs without NOM (top left). Dark-field micrographs of citrate-capped AgNPs are shown on the left; these are stabilized with the NOM type indicated. In the images on the right, bright features correspond to areas within the micrographs on the left that have high spectral similarity to NOM-free nanoparticles. An increasing number of bright pixels indicates increasing similarity between the spectral features of the NOM-stabilized nanoparticle and those of NOM-free nanoparticles (i.e., increasing similarity to heavily aggregated AgNPs). Pixel colors represent distinct wavelengths (within the UV-visible region) at which spectral matches were recorded.

Theoretical Responses of Ag^+ ISEs:

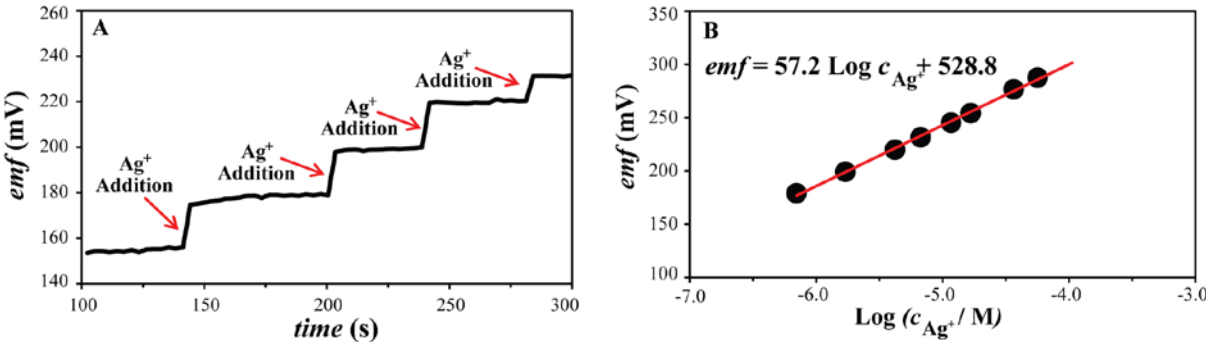

Figure S4: Representative calibration curve of a fluorous-phase Ag^+ ISE. (A) Red arrows indicate additions of aliquots of 10.0 mM $AgCH_3COO$ to the measuring solution. The emf of fluorous-phase Ag^+ ISEs increases after each Ag^+ addition. Only a portion of the calibration curve is shown for better visualization. (B) The linear relationship between the emf and Log c(Ag^+) can be used as the calibration equation for converting emf values to [Ag^+].

Potentiometric measurements are performed by the determination of the electrical potential (typically referred to as electromotive force, emf) between the measuring electrode (here the fluorous-phase Ag^+ ISE) and a reference electrode, which are both in contact with the sample of interest. Note that the reference electrode provides a constant, sample-independent contribution to the measured emf. Ideally, the emf gives a response that can be described with the Nernst equation, i.e., emf = E^o + (2.303 R T F^{-1}) Log a (Ag^+), where T represents the temperature in Kelvin, F is the Faraday constant, and R is the universal gas constant. For example, at 20 °C a tenfold increase in the Ag^+ activity results in a 58.2 mV increase in the measured emf.[3] Calibration of the ISEs to determine the constant E^o and check the prelogarithmic term (i.e., the response slope in a plot of emf vs Log a (Ag^+)) may be performed by addition of aliquots of concentrated $AgCH_3COO$ solution (*aq*) to a more dilute solution and measurement of the emf. The emf response of an electrode to Ag^+ addition provides the calibration curve resulting from

that data. Note that the activity of an ion is the product of the ion concentration and an activity coefficient, which depends, in general, on the ionic composition of the sample solution. However, in solutions with a fixed ionic strength, the activity coefficient of Ag^+ can be assumed to be constant and a plot of the emf vs Log *c* (Ag^+) exhibits the same linearity as the plot of the emf vs Log *a* (Ag^+). Therefore, emf data measured with a calibrated electrode can be converted to concentration using the calibration equation experimentally determined for that electrode. Figure S4 demonstrates the ISE-measured response to Ag^+ additions to buffer (panel A), and the corresponding calibration curve (panel B).

ISE-measured Dissolution of Citrate-capped AgNPs in pH Buffer Containing 10 mg/L NOM

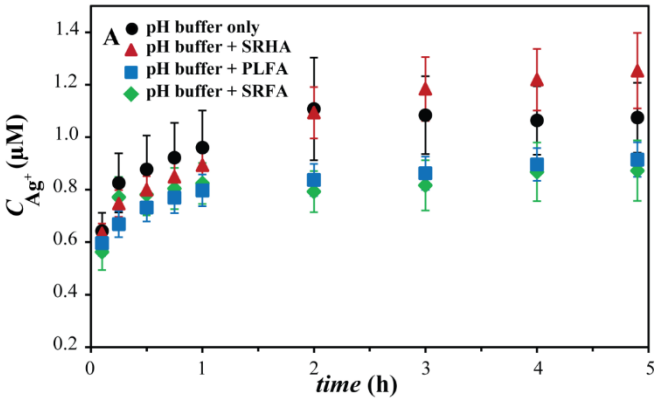

Figure S5. No significant effect of NOM on release of Ag^+ from 5 mg Ag/L citrate-capped AgNPs was observed at low NOM concentrations (10 mg/L) relative to NOM-free solutions. The Ag^+ released was measured with fluorous-phase Ag^+ ISEs in pH = 7.5 buffer with 10 mg/L SRHA, PLFA, or SRFA. Error bars represent the standard deviation of six replicate measurements.

ISE-measured Complexation of Ag^+ and Citrate or Polyvinylpyrrolidone

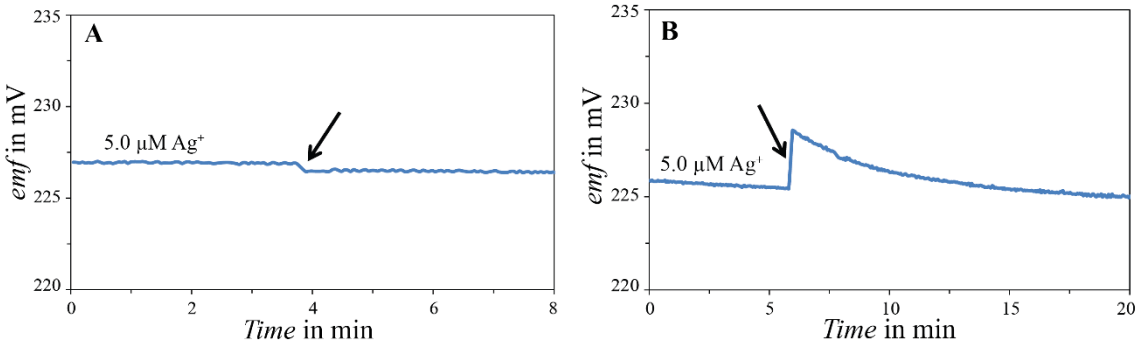

Figure S6. The emf of fluorous-phase Ag^+ ISEs in 5.0 µM $AgNO_3$ was monitored. (A) Addition of 50 mg/L trisodium citrate occurred at the time indicated by the black arrow and led to a 2% decrease in the Ag^+ concentration. (B) Addition of 50 mg/L polyvinylpyrrolidone (PVP-10) occurred at the time indicated by the black arrow, leading to an emf spike. After equilibration, no significant change in the Ag^+ concentration was observed.

Materials and Methods

Nanoparticle Synthesis:

Citrate-capped AgNPs were synthesized according to the method used by Hackley and coworkers.[4] All glassware was washed with aqua regia (3:1 HCl: HNO_3) and rinsed three times with deionized water (18 MΩ·cm specific resistance, EMD Millipore, Burlington, MA, USA) prior to use. First, 100 mL deionized water was brought to a boil. Then 365 µL of 34 mM trisodium citrate dihydrate (Sigma Aldrich, St. Louis, MO, USA) and 211 µL of 58.8 mM $AgNO_3$ (Sigma Aldrich, St. Louis, MO, USA) were added with constant stirring. After 30 seconds, 250 µL of freshly prepared 100 mM aqueous $NaBH_4$ was added drop-wise, and the mixture was boiled with constant stirring for 15 minutes. The mixture was then removed from heat and allowed to cool to room temperature before beginning purification. To remove synthesis by-products and purify the nanoparticles, 15 mL aliquots of the mixture were loaded into regenerated cellulose (MWCO 50,000) centrifugal filter units (EMD Millipore, Carrigtwohill, Ireland), centrifuged 4 minutes at 1500 RCF, and then resuspended in 15 mL deionized water. Centrifugation and resuspension were repeated two more times. Following the final resuspension in deionized water, the mixture was centrifuged a final time to concentrate the nanoparticles. Nanoparticle concentration in units of silver mass per volume was determined by measuring the UV-visible extinction spectrum (USB2000, Ocean Optics, Dunedin, FL, USA) using the nanoparticle extinction coefficient and silver atom number value reported by Maurer-Jones et al.[5]

Polyvinylpyrrolidone-capped AgNPs were prepared from the above citrate-capped AgNPs through ligand exchange, thus ensuring that nanoparticle core size and shape were preserved. Prior to centrifugal purification, a room temperature AgNP suspension, prepared as described above, was centrifuged for 30 minutes at 12500 RCF to pellet the nanoparticles. The supernatant was removed, replaced with 26 g/L PVP-10 (Sigma Aldrich, St. Louis, MO, USA),

and incubated at room temperature in the dark with constant stirring for four days. The AgNP suspension was then purified using centrifugal filter units as described above.

Nanoparticle Characterization:

Transmission Electron Microscopy (TEM):

Room temperature TEM images of AgNPs were acquired with a FEI Tecnai T12 microscope (FEI, Inc., Hillsboro, OR) operating at 120 kV. A 200 mesh copper grid with Formvar and carbon supports was dipped into a ~0.3 mg/mL NP suspension, then removed and allowed to dry before imaging. Image analysis was performed in ImageJ.[6]

Zeta Potential Measurement:

The zeta potential of citrate- and PVP-capped AgNPs was measured using a Brookhaven ZetaPALS Zeta-Potential and Particle Sizing Analyzer (Holtsville, NY). Three independent samples were prepared by diluting the purified nanoparticle suspensions to 5 mg Ag/L in deionized water (pH 6).

Buffer Preparation:

The buffer used in all nanoparticle stability and dissolution experiments was prepared by combining 0.028 M K_2HPO_4 and 0.015 M KH_2PO_4 in deionized water and adjusting the pH to 7.5 by KOH additions.

UV-vis Extinction Spectroscopy:

The AgNP aggregation state was tracked over 46 hours at room temperature by monitoring light extinction in the UV-visible range caused by the localized surface plasmon resonance (LSPR) effect using an OceanOptics USB2000 spectrometer coupled to a MicroPack DH-2000 UV-vis-NIR light source. Deionized water or deionized water with 10 mg/L NOM served as the blank references, and measurements were performed on two independent samples.

Dynamic Light Scattering Measurement:

The Z-average particle size of citrate- and PVP-capped AgNPs was measured over 196 hours using a Brookhaven ZetaPALS Zeta-Potential and Particle Sizing Analyzer (Holtsville, NY). Three independent samples were analyzed using three analytical replicates per sample.

Dark-field Microscopy and Hyperspectral Imaging:

While dark-field microscopy provides only qualitative information regarding AgNP stability, when performed in conjunction with hyperspectral imaging, it offers a semi-quantitative method to assess particle stability. In this work, hyperspectral scans consisting of hundreds of visible-near-infrared spectra were acquired within the field of view of a given dark-field image. These spectra are generated exclusively from light scattered at the nanoparticle surface and not absorbed light, since oblique-angle illumination is used. Scattered light intensity is dependent on the resonance frequency of localized surface plasmons at the nanoparticle surface, which in turn is dependent on the material dielectric properties (or refractive index), size, shape, and interparticle spacing. Aggregation of AgNPs results in a significant change in the localized surface plasmon resonance frequency (see Figure 1 in the main text), leading to shifts in hyperspectral features.

Hyperspectral scans acquired within the field of view of a given dark-field image were pooled into spectral libraries characteristic of each AgNP type (i.e., with different types of NOM). Spectral libraries of different nanoparticle conditions were compared using Spectral Angle Mapping similarity analysis software (ENVI 4.8, Exelis Visual Information Solutions, Boulder, CO). This similarity analysis yields plots (see Figure S3, right-hand side) in which the x- and y-axes indicate position within a corresponding dark-field image, and the pixel brightness indicates spectral matches to a reference sample (here, AgNPs without NOM) above a defined threshold (here, 95% spectral similarity). No further normalization of these data are required, since the relative fraction of bright pixels (in the similarity plots) to total nanoparticles (in the dark-field images) indicates the degree of similarity between AgNPs exposed to NOM and pristine AgNPs in the reference sample.

Dark-field micrographs of AgNPs exposed to NOM were acquired on an Olympus BX43 microscope (Olympus America, Inc., Center Valley, PA) modified with a high signal-to-noise darkfield condenser unit from CytoViva (Auburn, AL). A 3 µL sample aliquot was loaded onto a glass slide, covered with a coverslip, and imaged using a 150 W quartz-halogen lamp (Fiber-Lite DC-950, Dolan-Jenner Industries, Boxborough, MA), 100x 1.3 NA oil-immersion objective, and 12 bit CCD camera (pco.pixelfly, PCO, Kelheim, Germany). A hyperspectral imaging system consisting of a spectrophotometer (Specim, Oulu, Finland) and spectrophotometer-integrated CCD (pco.pixelfly, PCO, Kelheim, Germany) was then used to acquire hyperspectral images within the same field of view as the dark-field image.

Fabrication of Ag^+-Selective Electrodes with Fluorous Sensing Membranes:

Ion-selective electrodes (ISEs) were fabricated as reported.[7] Sensing phases were prepared by adding 0.5 mM ionic sites (sodium tetrakis[3,5-bis(perfluorohexyl)phenyl]borate) and 1.5 mM ionophore (1,3-bis(perfluorooctyl-ethylthiomethyl)benzene)[8] into perfluoroperhydrophenanthrene (Alfa Aesar, Ward Hill, MA, USA). The mixture that resulted was stirred for at least a day to make sure that all the membrane components were completely dissolved. Fluoropore™ filters (porous poly(tetrafluoroethylene), 47 mm diameter, 0.45 µm pore size, 50 µm thickness, 85% porosity) from EMD Millipore (Bedford, MA, USA) were placed between two sheets of paper and cut with a 13-mm-diameter hole punch. This gave porous filter disks that were then used to mechanically support the sensing phase. Approximately 25 µL of this sensing phase was subsequently placed onto a stack of 2 porous filter disks. Complete penetration of the sensing phase into the porous supports was indicated by translucence of the filter disks.

The sensing membranes (i.e., the filter disks infiltrated with the fluorous sensing phase) were then mounted into custom-machined electrode bodies (prepared in house from poly(chlorotrifluoroethylene), as reported previously).[8] For this purpose, a cap with a hole (8.3 mm diameter) in its center was screwed onto the electrode body, which positioned the sensing membrane between the cap and the electrode body but left all but the edge of the membrane exposed. Inner filling solution, 1 µM $AgCH_3CO_2$ (Sigma Aldrich, USA), was filled into the electrode bodies, and a AgCl-coated silver wire was inserted into this solution to act as the inner reference electrode. To replace the sodium ions in the thus prepared sensing membranes with silver ions, all electrodes were soaked prior to measurements for one day in 100 mL 0.1 mM $AgCH_3CO_2$ solution and then for another day in 100 mL 1.0 µM $AgCH_3CO_2$. This process is typically referred to as membrane conditioning.

Experimental Details of the Potentiometric Measurements:

An EMF 16 potentiometer (Lawson Labs, Malvern, PA, USA) with EMF Suite 1.02 software (Lawson Labs) was used for all potentiometric measurements, which were performed at room temperature in stirred solutions. The external reference electrode (relative to which all measurements with fluorous membrane ISEs were performed) was a double-junction AgCl/Ag electrode with a AgCl saturated 3.0 M KCl reference electrolyte and 1.0 M LiOAc bridge electrolyte. All measurements were performed as at least 3 replicates. Successive addition of aliquots of 10 mM $AgCH_3CO_2$ solution to deionized water or the pH buffers was used to provide the data for calibration curves.

For the observation of nanoparticle dissolution, three ISEs were fabricated, calibrated, and inserted into 100 mL of the solution in which dissolution was going to take place. AgNPs were purified as described above and were added to the solution of interest to give AgNP concentrations of 5 mg Ag/L. Sensor monitoring was performed for 5 hours. All electrodes were calibrated once more after the NOM additions to confirm that the electrodes still exhibited stable responses to Ag^+.

Bacterial Membrane Integrity Assay:

Bacterial membrane integrity was evaluated after AgNP exposure using the LIVE/DEAD Baclight Viability Kit (Product L-7012, Life Technologies). Cells cultured in LB broth were centrifuged at 2000 rcf for 10 minutes and resuspended at a concentration of 2×10^8 cells/mL in pH 7.5 phosphate buffer. Then 1 mL of cell suspension was mixed with purified citrate- or PVP-capped AgNPs (5 mg Ag/L) that had been incubated overnight with or without NOM as described in the Materials and Methods. After 30 minutes of room temperature incubation, cells were centrifuged at 2000 rcf for 10 minutes, the supernatant was removed, and cells were resuspended in pH 7.5 phosphate buffer. Then 100 µL of each sample was mixed with 100 µL of

a mixture of 3.34 mM Syto-9 and 20 mM propidium iodide provided in the Baclight Viability Kit in a 96 well plate. After a 15 minute room temperature incubation, fluorescence emission intensities at 528/20 nm (Syto-9 emission) and 635/32 nm (propidium iodide emission) were measured on a Synergy 2 Multi-Mode Reader (BioTek, Winooski, VT) using an excitation wavelength of 485/20 nm. The response of cells exposed to NOM in the absence of AgNPs (at a concentration matching that present in samples exposed to AgNPs pre-incubated with NOM) was not significantly different from that of the negative control (cells exposed to neither AgNPs nor NOM).

References

(1) Nath, S.; Ghosh, S. K.; Kundu, S.; Praharaj, S.; Panigrahi, S.; Pal, T. Is Gold Really Softer than Silver?: HSAB Principle Revisited. *J. Nanoparticle Res.* **2006**, *8*, 111–116.
(2) Elemental Compositions and Stable Isotopic Ratios of IHSS Samples.
(3) Buhlmann, P.; Chen, L. D. Ion-Selective Electrodes With Ionophore-Doped Sensing Membranes. In *Supramolecular Chemistry: From Molecules to Nanomaterials*; Wiley, 2012; pp. 2539–2579.
(4) Chinnapongse, S., L.; MacCuspie, R. I.; Hackley, V. A. Persistence of Singly Dispersed Silver Nanoparticles in Natural Freshwaters, Synthetic Seawater, and Simulated Estuarine Waters. *Sci. Total. Environ.* **2011**, *409*, 2443–2450.
(5) Maurer-Jones, M. A.; Mousavi, M. P. S.; Chem, L. D.; Buhlmann, P.; Haynes, C. L. Characterization of Silver Ion Dissolution from Silver Nanoparticles Using Fluorous-Phase Ion-Selective Electrodes and Assessment of Resultant Toxicity to *Shewanella Oneidensis*. *Chem. Sci.* **2013**, *4*, 2564–2572.
(6) Schneider, C. A.; Rasband, W. S.; Eliceiri, K. W. NIH Image to ImageJ: 25 Years of Image Analysis. *Nat. Methods* **2012**, *9*, 671–675.
(7) Lai, C.-Z.; Fierke, M. A.; Corrêa da Costa, R.; Gladysz, J. A.; Stein, A.; Bühlmann, P. Highly Selective Detection of Silver in the Low Ppt Range with Ion-Selective Electrodes Based on Ionophore-Doped Fluorous Membranes. *Anal. Chem.* **2010**, *82*, 7634–7640.
(8) Boswell, P. G.; Bühlmann, P. Fluorous Bulk Membranes for Potentiometric Sensors with Wide Selectivity Ranges: Observation of Exceptionally Strong Ion Pair Formation. *J. Am. Chem. Soc.* **2005**, *127*, 8958–8959.